

Selective Substrate-Orbital-Filtering Effect to Realize the Large-Gap Quantum Spin Hall Effect

Huisheng Zhang, Yingying Wang, Wenjia Yang, Jingjing Zhang, Xiaohong Xu,* and Feng Liu*

Cite This: *Nano Lett.* 2021, 21, 5828–5833

Read Online

ACCESS |

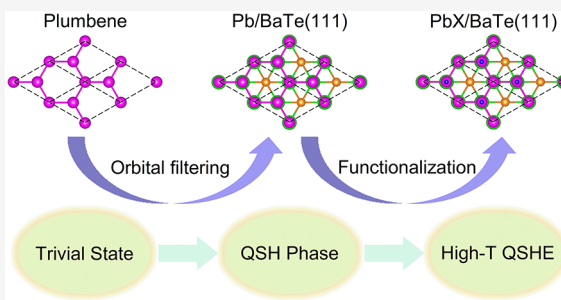
Metrics & More

Article Recommendations

Supporting Information

ABSTRACT: Although Pb harbors a strong spin–orbit coupling effect, pristine plumbene (the last group-IV cousin of graphene) hosts topologically trivial states. Based on first-principles calculations, we demonstrate that epitaxial growth of plumbene on the BaTe(111) surface converts the trivial Pb lattice into a quantum spin Hall (QSH) phase with a large gap of ~ 0.3 eV via a *selective* substrate-orbital-filtering effect. Tight-binding model analyses show the p_z orbital in half of the Pb overlayer is selectively removed by the BaTe substrate, leaving behind a p_z – $p_{x,y}$ band inversion. Based on the same working principle, the gap can be further increased to ~ 0.5 – 0.6 eV by surface adsorption of H or halogen atoms that filters out the other half of the Pb p_z orbitals. The mechanism of *selective* substrate-orbital-filtering is general, opening an avenue to explore large-gap QSH insulators in heavy-metal-based materials. It is worth noting that plumbene has already been widely grown on various substrates experimentally.

KEYWORDS: Plumbene, substrate-orbital-filtering effect, quantum spin Hall insulator, first-principles calculations, tight-binding model



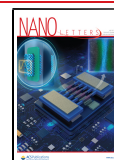
The quantum spin Hall (QSH) effect^{1,2} has attracted increasing research attention because of its fundamental interest and promising potential applications in quantum computing and spintronics devices. This two-dimensional (2D) topological state was first proposed by Kane and Mele in graphene, where spin–orbit coupling (SOC) can, in principle, open a nontrivial bandgap at the Dirac point, within which two helical edge states reside.³ However, the SOC of C is negligibly small (in the order of 10^{-3} meV),⁴ rendering graphene practically a semimetal rather than a QSH insulator. The first experimentally confirmed QSH insulator is the HgTe quantum well,^{5,6} which has a very small gap. Since then, many 2D QSH insulators,^{7–26} some with a large gap, have been theoretically predicted and a few experimentally confirmed, including, e.g., HgTe/CdTe QWs,⁶ InAs/GaSb QWs,²⁷ Bi bilayer,²⁸ and 1T' WTe₂ monolayer.^{29–31}

Realization of large-gap (and hence possibly high-temperature) QSH insulators is expected to be one of the key milestones in the field of topological materials for practical applications. A natural system that comes to mind is one made of only heavy metal elements of large SOC. For example, it has been predicted that epitaxial growth of bismuthene on hydrogenated and halogenated Si(111) substrates can realize a large-gap QSH phase via an interesting substrate-orbital-filtering effect,^{16,17} and the idea has been further applied to SiC and Ge substrates.^{32,33} Shortly after, employing this idea, bismuthene has been grown experimentally on the H-SiC substrate, showing a large gap of ~ 0.8 eV by scanning tunneling microscopy.³⁴ However, the quantized transport, the most critical signature of the QSH effect, has not been

demonstrated for this system. Therefore, discovering elemental 2D layers exhibiting a large-gap QSH effect remains still a high-order challenge. In this Letter, we propose plumbene as a promising candidate.

By performing first-principle calculations, we first show that both planar and low-buckled plumbene host topologically trivial states due to the coexistence of nontrivial quadratic and Dirac bands that act together destructively, in agreement with previous works.^{25,26} Then, we demonstrate that epitaxial growth of plumbene on the BaTe(111) surface will convert the topologically trivial Pb lattice into a large-gap (~ 0.3 eV) QSH insulator by a *selective* substrate-orbital-filtering effect, as revealed by first-principles and tight-binding (TB) model analyses. Specifically, the p_z orbitals in half of the Pb overlayer are found to be selectively removed by the BaTe substrate, resulting in a p_z – $p_{x,y}$ band inversion. Furthermore, an even larger gap of ~ 0.5 – 0.6 eV can be achieved when the other half of Pb atoms are surface adsorbed with H or halogen atoms, based on the same orbital-filtering mechanism. These results indicate that BaTe(111) film affords an ideal substrate to realize a large-gap QSH effect in elemental plumbene.

Received: May 5, 2021
Revised: June 16, 2021
Published: June 22, 2021



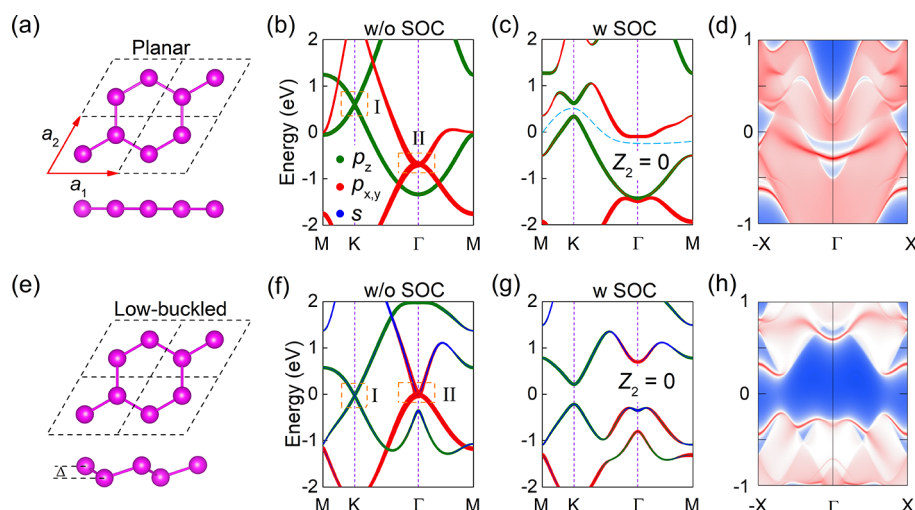


Figure 1. (a) Top and side views of a 2×2 supercell for planar plumbene. a_1 and a_2 are basis vectors of the unit cell. Calculated band structures of planar plumbene without (b) and with (c) SOC, respectively. The Fermi level is set to zero. The blue dashed line in part c denotes the “curved” Fermi level. The projected bands of Pb s , $p_{x,y}$, and p_z orbitals are also given. (d) Edge states of planar plumbene. (e–h) The same as parts a–d for low-buckled plumbene. Regions I and II in parts b and f indicate the Dirac and quadratic bands, respectively. Δ in part e is the buckling height of the low-buckled plumbene.

2D hexagonal lattices of group-IV elements (C,³ Si,⁷ Ge,⁸ Sn,^{9,22} and Pb^{25,26}) have attracted much interest as a prototypical model system for studying the QSH effect. The ones made of light elements, such as C and Si, are topologically nontrivial but have too small a SOC, while the one made of the heaviest element, i.e., Pb, has a larger SOC but is topologically trivial. This trend of changing band topology is caused by the change of orbital composition of bands at the Fermi level. As one goes down the group-IV column, the s – p level splitting increases and hence the s – p hybridization decreases. At the limit of C, there is a strong sp^2 hybridization forming six gapped valence and conduction bands, leaving the remaining p_z orbital to form two middle half-filled π bands, i.e., the Dirac bands of nontrivial topology. At the limit of Pb, there is a negligible sp hybridization so that three (p_x , p_y , p_z) orbitals form six p bands around the Fermi level, leading to trivial topology.³⁵

More specifically, we show the calculated band structures and band topology of freestanding planar and low-buckled hexagonal plumbene in Figure 1. The planar plumbene has an optimized lattice constant of 5.14 Å (Figure 1a). Its band structure without SOC is shown in Figure 1b, having two metallic p bands crossing the Fermi level. With SOC, the four valence bands are separated from the four conduction bands (only two around the Fermi level are shown for each group in Figure 1c) by a “curved” gap (indicated by the blue dashed line within the gap), and one can calculate the topological invariant from the Wannier charge center (WCC) by assuming occupying only all of the valence bands. This leads to $Z_2 = 0$ (Figure S1), indicating that freestanding plumbene is topologically trivial. Edge state calculations with SOC confirm that there is no edge state in the curved gap, as displayed in Figure 1d.

It is well-known that two structures belong to the same topological class if they are adiabatically connected.³⁶ Thus, when the planar plumbene buckles, there will be no change of topology as long as there is no band crossing. This is what happens, as shown in Figure 1e–h. Although the system remains trivial, one notices that the buckling opens a global

gap of 0.43 eV with SOC (Figure 1g) by fully separating the valence and conduction bands (Figure 1c,d vs g,h). This global gap turns out to be critically important to facilitate the *selective* substrate-filtering effect that converts the system into a topological nontrivial state, as discussed later.

There are six p bands around the Fermi level, which together make the system overall trivial. If there were only p_z^3 or (p_x , p_y) orbitals^{37,38} in a hexagonal lattice, the system would be nontrivial. Therefore, one approach to make such a system be topological is to remove the p_z orbital from the Fermi level, as shown by the so-called substrate-orbital-filtering effect for bismuthene grown on a semiconductor substrate.¹³ For the case of planar bismuthene, the three p orbitals are “perfectly” degenerate at the Fermi level, and one needs to remove the p orbital from every Bi atom in the hexagonal lattice. Here we found that, to convert the plumbene into a QSH insulator, one needs only to remove the p orbital from half of the Pb atom in the lattice, which we dubbed as a *selective* substrate-orbital-filtering effect.

It is worth noting that epitaxial growth of ultrathin Pb films on metallic and semiconductor substrates has already attracted much interest for a long time in the context of the quantum size effect^{39,40} and superconductivity,⁴¹ including “plumbene”,⁴² before the emergence of topological materials. This makes experimental realization of topological plumbene highly feasible if a suitable system can be predicted. And recent works of growing plumbene on $\text{Pd}_{1-x}\text{Pb}_x(111)$ and $\text{Fe}/\text{Ir}(111)$ substrates^{43,44} and intercalating Pb between the graphene and Pt surface further strengthens this possibility.⁴⁵ However, the metallic substrates likely render the Pb overlayer topologically trivial. We believe the key is to find a right substrate, which has motivated the present work.

There are several considerations in the order. First, a semiconductor or insulator substrate is needed to avoid overlapping the overlayer topological states by the substrate electronic states. Second, a close lattice match between the overlayer and substrate is preferred to minimize interface strain. Last and most critical, a viable physical mechanism can be exploited to convert the trivial freestanding plumbene into a

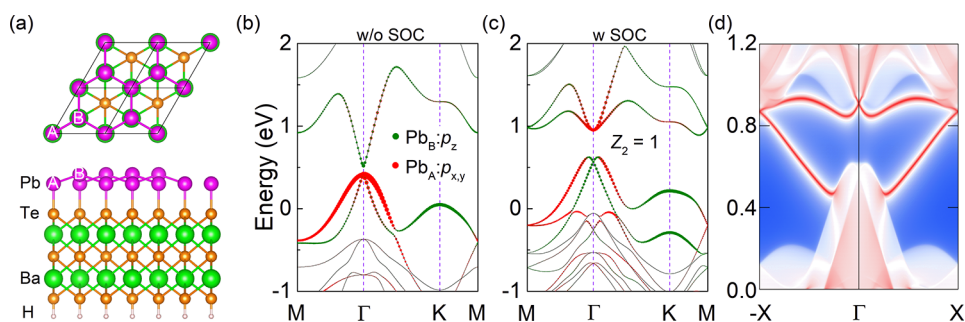


Figure 2. (a) Top and side views of a 2×2 supercell for BaTe(111)-supported low-buckled plumbene. A and B represent two sublattices of plumbene. The band structures without (b) and with (c) SOC, respectively. The projected bands of Pb p_{xy} and p_z orbitals are also shown. (d) Calculated edge states of Pb-BaTe(111).

topological phase and preferably with a larger SOC gap. Here, we identify BaTe(111) to be such a substrate to meet all three conditions. BaTe is an insulator having a band gap of ~ 3.4 eV.⁴⁶ The lattice constant of the BaTe(111) surface is ~ 4.95 Å,⁴⁷ which matches perfectly with that of low-buckled plumbene (~ 4.93 Å). Below, we demonstrate that it can indeed convert plumbene into a large-gap QSH insulator via a *selective* substrate-orbital-filtering mechanism, as an extension to the similar effect that converts bismuthene into topological on a semiconductor substrate.¹³

Different from the planar plumbene grown on the metallic substrates,^{43,44} we found that the plumbene adopts the low-buckled stable structure when grown on the BaTe(111) surface, as displayed in Figure 2a. To assess the thermodynamic stability of the proposed overlayer structure, we first calculated the surface energy of the BaTe(111) substrate, which is ~ 71 meV/Å², and then the surface/interface energies of the Pb/BaTe(111) overlayer, which is ~ 60 meV/Å². Both of these values are relatively low, e.g., in comparison with the Si(111) surface energy of ~ 90 meV/Å²,⁴⁸ indicating their high stability. Also, no reconstruction was found in both surfaces after structural optimization. On the other hand, growth kinetics, such as rates of nucleation and diffusion, is important, which should be explored in the future.

The band structure of the Pb-BaTe(111) without SOC is shown in Figure 2b. In comparison with the band structure of freestanding plumbene, one notices that the Dirac bands around the K (K') point in Figure 1b or f are completely removed, because the p_z orbital on the lower Pb atoms (namely, the A sites in Figure 2a) is selectively removed by the surface Te atoms of the BaTe substrate. There is a 0.11 eV bandgap at the Γ point above the Fermi level. From the orbital projected bands in Figure 2b, one can see that the “valence” bands below the gap are mainly contributed by the p_{xy} orbitals of the lower A-site Pb atoms, whose p_z orbitals are filtered out, while the “conduction” bands above the gap are contributed by the p_z orbitals of the upper B-site Pb atoms in the substrate-supported plumbene. After SOC is considered, a ~ 0.27 eV band gap opens, signifying clearly a p_{xy} - p_z band inversion, as shown in Figure 2c. The nontrivial topology is confirmed by the calculated topological invariant, $Z_2 = 1$ and edge states shown in Figure 2d. Thus, the Pb-BaTe(111) is predicted a large-gap QSH system via a *selective* substrate-orbital-filtering effect where the p_z orbitals on half of the Pb atoms are removed by the substrate.

Next, we employ a three-band spinless tight-binding (TB) model to better reveal the underlying physical mechanism of the *selective* substrate-orbital-filtering effect in Pb-BaTe(111).

Based on the above first-principles results, the TB model is constructed by using two p_{xy} orbitals on A sites and one p_z orbital on B sites as basis,⁴⁹ and the Hamiltonian can be written as $H(k) = H_{\text{hop}}(k) + H_{\text{SOC}}$, where H_{hop} represents the nearest-neighbor (NN) hopping and H_{SOC} is the on-site SOC. The detailed expressions of $H(k)$ are given in the Supporting Information. The resulting TB band structure without SOC is shown in Figure 3a, which captures the main features of DFT

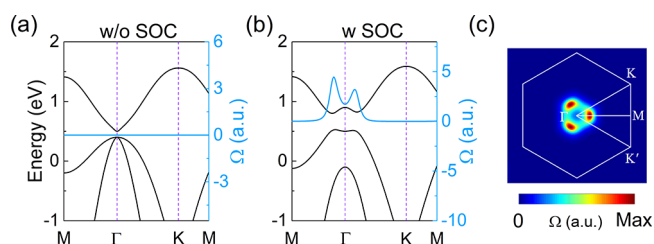


Figure 3. Electronic band structures along the high-symmetry path without (a) and with (b) SOC obtained from the tight-binding model. Here, the detailed parameters are shown in the Supporting Information. The blue lines in parts a and b denote the 1D Berry curvatures. (c) Corresponding distribution of 2D Berry curvatures in the first Brillouin zone.

bands in Figure 2b. Adding SOC, an inverted gap opens as expected (Figure 3b). Also, detailed information on 1D and 2D Berry curvature distribution⁵⁰ is given in Figure 3b,c, from which the Chern number, $C = 1$ is obtained. The nonzero Berry curvature is located around the Γ point.

Based on the same working principle, we also found that the QSH state in the as-grown Pb-BaTe(111), as shown above, can be further enhanced with a larger gap, by surface adsorption with H or halogen atoms. Figure 4a shows the top and side views of the resulting PbX-BaTe(111) system, whose structural properties are summarized in Table 1. Upon hydrogenation or halogenation, the p_z orbitals on the other half of Pb atoms (B sites in Figure 2a) are also removed. This leaves only p_{xy} orbitals around the Fermi level, as illustrated by the calculated band structures of PbH-BaTe(111), shown in Figure 4 as an example. Without SOC (Figure 4b), there are two touching quadratic p_{xy} bands at the Fermi level, representing a semimetal. With SOC (Figure 4c), a global bandgap of 0.52 eV is opened, indicating a large-gap QSH state formed via a type of band inversion between $p_x + ip_y$ and $p_x - ip_y$ orbitals.²⁰ Figure 4d shows clearly two helical edge states in the bulk gap. Similar results are obtained in the halogenated Pb-BaTe(111) system (Figure S2) with a gap ranging from 0.45 to 0.55 eV, which are increased to ~ 0.5 – 0.6 eV by using the hybrid

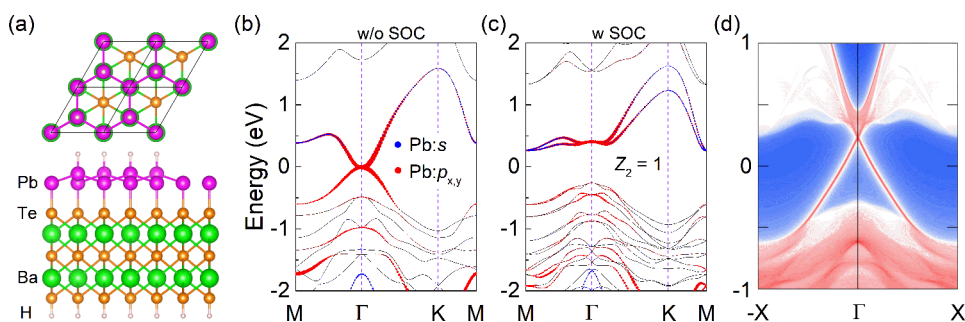


Figure 4. (a) Top and side views of the 2×2 supercell for PbX/BaTe(111), where X = H, F, Cl, Br, or I. The band structures without (b) and with (c) SOC, respectively. The projected bands of Pb $p_{x,y}$ and s orbitals are also shown. (d) Calculated edge states of PbH/BaTe(111).

Table 1. Structural, Electronic, and Topological Properties of Pb/BaTe(111) and PbX/BaTe(111) (X = H, F, Cl, Br, or I), Where $d_{\text{Pb-Pb}}$, $d_{\text{Pb-X}}$, and $d_{\text{Pb-Te}}$ Represent the Distances of Pb–Pb, Pb–X, and Pb–Te, Respectively, and $E_{\text{g-DFT}}$ and $E_{\text{g-HSE}}$ Denote the Nontrivial Bandgaps Obtained from DFT and HSE06 Calculations

X	Δ (Å)	$d_{\text{Pb-Pb}}$ (Å)	$d_{\text{Pb-X}}$ (Å)	$d_{\text{Pb-Te}}$ (Å)	$E_{\text{g-DFT}}$ (eV)	$E_{\text{g-HSE}}$ (eV)	Z_2
Pb/BaTe(111)	1.15	3.06		2.88	0.27	0.32	1
H	0.87	2.99	1.85	2.84	0.52	0.61	1
F	0.77	2.96	2.08	2.85	0.55	0.61	1
Cl	0.84	2.98	2.48	2.85	0.51	0.56	1
Br	0.86	2.98	2.62	2.85	0.49	0.54	1
I	0.88	2.99	2.82	2.85	0.45	0.51	1

functional HSE06 method,⁵¹ as listed in Table 1. We have also considered another configuration of Pb–BaTe(111) and PbX–BaTe(111) (Figures S3 and S4), indicating the robustness of their topological order.

Finally, we further examined the thermodynamic stability of the Pb–BaTe(111) system at room temperature, by performing *ab initio* molecular dynamics (AIMD) simulations at 300 K. In the AIMD simulations, we double the supercell size to allow the surface to reconstruct more freely. A canonical ensemble was adopted with the Nosé thermostat⁵² and a time step of 1.0 fs. The ordered structure is seen to remain stable (intact) after 10 ps of simulation (Figure S5).

In summary, we propose the insulating BaTe(111) surface as an ideal substrate to grow plumbene, to achieve a large-gap QSH insulator. Our theoretical calculations and analyses reveal that the topologically trivial freestanding plumbene is converted into a QSH phase by a *selective* substrate-orbital-filtering effect. Furthermore, the topological gap can be increased significantly when the outermost Pb atoms of plumbene are hydrogenated or halogenated. We envision that the *selective* substrate-orbital-filtering effect may provide a general mechanism for realizing the high-temperature QSH effect in other heavy-metal-based systems and the high-temperature quantum anomalous effect in transition-metal-based systems.

ASSOCIATED CONTENT

Supporting Information

The Supporting Information is available free of charge at <https://pubs.acs.org/doi/10.1021/acs.nanolett.1c01765>.

Additional information on the details of first-principles calculations, the tight-binding model, and electronic and topological properties of PbX–BaTe(111) (PDF)

AUTHOR INFORMATION

Corresponding Authors

Xiaohong Xu – Key Laboratory of Magnetic Molecules and Magnetic Information Materials of Ministry of Education and Research Institute of Materials Science, Shanxi Normal University, Linfen 041004, China; orcid.org/0000-0001-7588-4793; Email: xuxh@sxnu.edu.cn

Feng Liu – Department of Materials Science and Engineering, University of Utah, Salt Lake City, Utah 84112, United States; orcid.org/0000-0002-3701-8058; Email: fliu@eng.utah.edu

Authors

Huisheng Zhang – Key Laboratory of Magnetic Molecules and Magnetic Information Materials of Ministry of Education and Research Institute of Materials Science, Shanxi Normal University, Linfen 041004, China; orcid.org/0000-0001-7369-9068

Yingying Wang – Key Laboratory of Magnetic Molecules and Magnetic Information Materials of Ministry of Education and Research Institute of Materials Science, Shanxi Normal University, Linfen 041004, China

Wenjia Yang – Key Laboratory of Magnetic Molecules and Magnetic Information Materials of Ministry of Education and Research Institute of Materials Science, Shanxi Normal University, Linfen 041004, China

Jingjing Zhang – Key Laboratory of Magnetic Molecules and Magnetic Information Materials of Ministry of Education and Research Institute of Materials Science, Shanxi Normal University, Linfen 041004, China

Complete contact information is available at: <https://pubs.acs.org/doi/10.1021/acs.nanolett.1c01765>

Notes

The authors declare no competing financial interest.

ACKNOWLEDGMENTS

This work was supported by the National Key R&D Program of China (Grant No. 2017YFB0405703), the National Natural Science Foundation of China (Grant Nos. 11804210, 51871137, and 61434002), and the Natural Science Foundation of Shanxi Province (China) (Grant No. 201901D211406). F.L. was supported by DOE-BES (DE-FG02-04ER46148).

REFERENCES

- (1) Hasan, M. Z.; Kane, C. L. Colloquium: Topological Insulators. *Rev. Mod. Phys.* **2010**, *82*, 3045–3067.
- (2) Qi, X. L.; Zhang, S. C. Topological Insulators and Superconductors. *Rev. Mod. Phys.* **2011**, *83*, 1057–1110.
- (3) Kane, C. L.; Mele, E. J. Quantum Spin Hall Effect in Graphene. *Phys. Rev. Lett.* **2005**, *95*, 226801.
- (4) Yao, Y. G.; Ye, F.; Qi, X. L.; Zhang, S. C.; Fang, Z. Spin-Orbit Gap of Graphene: First-Principles Calculations. *Phys. Rev. B: Condens. Matter Mater. Phys.* **2007**, *75*, No. 041401.
- (5) Bernevig, B. A.; Hughes, T. L.; Zhang, S. C. Quantum Spin Hall Effect and Topological Phase Transition in HgTe Quantum Wells. *Science* **2006**, *314*, 1757–1761.
- (6) König, M.; Wiedmann, S.; Brune, C.; Roth, A.; Buhmann, H.; Molenkamp, L. W.; Qi, X. L.; Zhang, S. C. Quantum Spin Hall Insulator State in HgTe Quantum Wells. *Science* **2007**, *318*, 766–770.
- (7) Liu, C. C.; Feng, W.; Yao, Y. G. Quantum Spin Hall Effect in Silicene and Two-Dimensional Germanium. *Phys. Rev. Lett.* **2011**, *107*, No. 076802.
- (8) Si, C.; Liu, J.; Xu, Y.; Wu, J.; Gu, B. L.; Duan, W. Functionalized Germanene as a Prototype of Large-Gap Two-Dimensional Topological Insulators. *Phys. Rev. B: Condens. Matter Mater. Phys.* **2014**, *89*, 115429.
- (9) Xu, Y.; Yan, B.; Zhang, H. J.; Wang, J.; Xu, G.; Tang, P.; Duan, W.; Zhang, S. C. Large-Gap Quantum Spin Hall Insulators in Tin Films. *Phys. Rev. Lett.* **2013**, *111*, 136804.
- (10) Liu, Z.; Liu, C. X.; Wu, Y. S.; Duan, W. H.; Liu, F.; Wu, J. Stable Nontrivial Z_2 Topology in Ultrathin Bi(111) Films: a First-Principles Study. *Phys. Rev. Lett.* **2011**, *107*, 136805.
- (11) Miao, M. S.; Yan, Q.; Van de Walle, C. G.; Lou, W. K.; Li, L. L.; Chang, K. Polarization-Driven Topological Insulator Transition in a GaN/InN/GaN Quantum Well. *Phys. Rev. Lett.* **2012**, *109*, 186803.
- (12) Kou, L.; Yan, B.; Hu, F.; Wu, S. C.; Wehling, T. O.; Felser, C.; Chen, C.; Frauenheim, T. Graphene-Based Topological Insulator with an Intrinsic Bulk Band Gap above Room Temperature. *Nano Lett.* **2013**, *13*, 6251–6255.
- (13) Zhou, M.; Ming, W. M.; Liu, Z.; Wang, Z.; Li, P.; Liu, F. Epitaxial Growth of Large-Gap Quantum Spin Hall Insulator on Semiconductor Surface. *Proc. Natl. Acad. Sci. U. S. A.* **2014**, *111*, 14378–14381.
- (14) Weng, H. M.; Dai, X.; Fang, Z. Transition-Metal Pentatelluride $ZrTe_5$ and $HfTe_5$: A Paradigm for Large-Gap Quantum Spin Hall Insulators. *Phys. Rev. X* **2014**, *4*, No. 011002.
- (15) Zhou, J. J.; Feng, W.; Liu, C. C.; Guan, S.; Yao, Y. Large-Gap Quantum Spin Hall Insulator in Single Layer Bismuth Monobromide Bi_4Br_4 . *Nano Lett.* **2014**, *14*, 4767–4771.
- (16) Zhou, M.; Liu, Z.; Ming, W.; Wang, Z.; Liu, F. sd^2 Graphene: Kagome Band in a Hexagonal Lattice. *Phys. Rev. Lett.* **2014**, *113*, 236802.
- (17) Zhou, M.; Ming, W.; Liu, Z.; Wang, Z.; Yao, Y.; Liu, F. Formation of Quantum Spin Hall State on Si Surface and Energy Gap Scaling with Strength of Spin Orbit Coupling. *Sci. Rep.* **2014**, *4*, 7102.
- (18) Qian, X.; Liu, J.; Fu, L.; Li, J. Quantum Spin Hall Effect in Two-Dimensional Transition Metal Dichalcogenides. *Science* **2014**, *346*, 1344–1347.
- (19) Huang, B.; Jin, K. H.; Zhuang, H. L.; Zhang, L.; Liu, F. Interface Orbital Engineering of Large-Gap Topological States: Decorating Gold on a Si(111) Surface. *Phys. Rev. B: Condens. Matter Mater. Phys.* **2016**, *93*, 115117.
- (20) Wang, Z. F.; Jin, K. H.; Liu, F. Quantum Spin Hall Phase in 2D Trigonal Lattice. *Nat. Commun.* **2016**, *7*, 12746.
- (21) Si, C.; Jin, K. H.; Zhou, J.; Sun, Z.; Liu, F. Large-Gap Quantum Spin Hall State in MXenes: d-Band Topological Order in a Triangular Lattice. *Nano Lett.* **2016**, *16*, 6584–6591.
- (22) Zhang, H.; Wang, Z.; Xu, X. Room Temperature Quantum Spin Hall Insulator: Functionalized Stanene on Layered PbI_2 Substrate. *Appl. Phys. Lett.* **2017**, *111*, No. 072105.
- (23) Wang, H.; Lu, D.; Kim, J.; Wang, Z.; Pi, S. T.; Wu, R. Q. Searching for Large-Gap Quantum Spin Hall Insulators: Boron-Nitride/(Pb,Sn)/ α - Al_2O_3 Sandwich Structures. *Nanoscale* **2017**, *9*, 2974–2980.
- (24) Li, C.; Jin, K. H.; Zhang, S.; Wang, F.; Jia, Y.; Liu, F. Formation of a Large Gap Quantum Spin Hall Phase in a 2D Trigonal Lattice with Three p-Orbitals. *Nanoscale* **2018**, *10*, 5496–5502.
- (25) Ma, Y.; Dai, Y.; Kou, L.; Frauenheim, T.; Heine, T. Robust Two-Dimensional Topological Insulators in Methyl-Functionalized Bismuth, Antimony, and Lead Bilayer Films. *Nano Lett.* **2015**, *15*, 1083–1089.
- (26) Yu, X. L.; Huang, L.; Wu, J. From a Normal Insulator to a Topological Insulator in Plumbene. *Phys. Rev. B: Condens. Matter Mater. Phys.* **2017**, *95*, 125113.
- (27) Knez, I.; Du, R. R.; Sullivan, G. Evidence for Helical Edge Modes in InAs/GaSb Quantum Wells. *Phys. Rev. Lett.* **2011**, *107*, 136603.
- (28) Yang, F.; Miao, L.; Wang, Z. F.; Yao, M. Y.; Zhu, F.; Song, Y. R.; Wang, M. X.; Xu, J. P.; Fedorov, A. V.; Sun, Z.; Zhang, G. B.; Liu, C.; Liu, F.; Qian, D.; Gao, C. L.; Jia, J. F. Spatial and Energy Distribution of Topological Edge States in Single Bi(111) Bilayer. *Phys. Rev. Lett.* **2012**, *109*, No. 016801.
- (29) Fei, Z.; Palomaki, T.; Wu, S.; Zhao, W.; Cai, X.; Sun, B.; Nguyen, P.; Finney, J.; Xu, X.; Cobden, D. H. Edge Conduction in Monolayer WTe_2 . *Nat. Phys.* **2017**, *13*, 677–682.
- (30) Tang, S.; Zhang, C.; Wong, D.; Pedramrazi, Z.; Tsai, H. Z.; Jia, C.; Moritz, B.; Claassen, M.; Ryu, H.; Kahn, S.; Jiang, J.; Yan, H.; Hashimoto, M.; Lu, D.; Moore, R. G.; Hwang, C. C.; Hwang, C.; Hussain, Z.; Chen, Y.; Ugeda, M. M.; Liu, Z.; Xie, X.; Devereaux, T. P.; Crommie, M. F.; Mo, S. K.; Shen, Z. X. Quantum Spin Hall State in Monolayer $1T'$ - WTe_2 . *Nat. Phys.* **2017**, *13*, 683–687.
- (31) Peng, L.; Yuan, Y.; Li, G.; Yang, X.; Xian, J. J.; Yi, C. J.; Shi, Y. G.; Fu, Y. S. Observation of Topological States Residing at Step Edges of WTe_2 . *Nat. Commun.* **2017**, *8*, 659.
- (32) Hsu, C. H.; Huang, Z. Q.; Chuang, F. C.; Kuo, C. C.; Liu, Y. T.; Lin, H.; Bansil, A. The Nontrivial Electronic Structure of Bi/Sb Honeycombs on SiC (0001). *New J. Phys.* **2015**, *17*, No. 025005.
- (33) Li, P.; Zhou, M.; Zhang, L.; Guo, Y.; Liu, F. Formation of a Quantum Spin Hall State on a Ge (111) Surface. *Nanotechnology* **2016**, *27*, No. 095703.
- (34) Reis, F.; Li, G.; Dudy, L.; Bauernfeind, M.; Glass, S.; Hanke, W.; Thomale, R.; Schäfer, J.; Claessen, R. Bismuthene on a SiC Substrate: A Candidate for a High-Temperature Quantum Spin Hall Material. *Science* **2017**, *357*, 287–290.
- (35) Li, Y.; Zhang, J.; Zhao, B.; Xue, Y.; Yang, Z. Constructive Coupling Effect of Topological States and Topological Phase Transitions in Plumbene. *Phys. Rev. B: Condens. Matter Mater. Phys.* **2019**, *99*, 195402.
- (36) Huang, H.; Liu, F. A Unified View of Topological Phase Transition in Band Theory. *Research* **2020**, *2020*, 7832610.
- (37) Wu, C.; Bergman, D.; Balents, L.; Das Sarma, S. Flat Bands and Wigner Crystallization in the Honeycomb Optical Lattice. *Phys. Rev. Lett.* **2007**, *99*, No. 070401.
- (38) Liu, Z.; Wang, Z. F.; Mei, J. W.; Wu, Y. S.; Liu, F. Flat Chern Band in a Two-Dimensional Organometallic Framework. *Phys. Rev. Lett.* **2013**, *110*, 106804.
- (39) Chan, T. L.; Wang, C. Z.; Hupalo, M.; Tringides, M. C.; Ho, K. M. Quantum Size Effect on the Diffusion Barriers and Growth Morphology of Pb/Si(111). *Phys. Rev. Lett.* **2006**, *96*, 226102.

- (40) Ma, L. Y.; Tang, L.; Guan, Z. L.; He, K.; An, K.; Ma, X. C.; Jia, J. F.; Xue, Q. K.; Han, Y.; Huang, S.; Liu, F. Quantum Size Effect on Adatom Surface Diffusion. *Phys. Rev. Lett.* **2006**, *97*, 266102.
- (41) Eom, D.; Qin, S.; Chou, M. Y.; Shih, C. K. Persistent Superconductivity in Ultrathin Pb Films: A Scanning Tunneling Spectroscopy Study. *Phys. Rev. Lett.* **2006**, *96*, No. 027005.
- (42) Qin, S.; Kim, J.; Niu, Q.; Shih, C. K. Superconductivity at the Two-Dimensional Limit. *Science* **2009**, *324*, 1314–1317.
- (43) Yuhara, J.; He, B.; Matsunami, N.; Nakatake, M.; Le Lay, G. Graphene's Latest Cousin: Plumbene Epitaxial Growth on a "Nano WaterCube". *Adv. Mater.* **2019**, *31*, 1901017.
- (44) Bihlmayer, G.; Sassmannshausen, J.; Kubetzka, A.; Blugel, S.; von Bergmann, K.; Wiesendanger, R. Plumbene on a Magnetic Substrate: A Combined Scanning Tunneling Microscopy and Density Functional Theory Study. *Phys. Rev. Lett.* **2020**, *124*, 126401.
- (45) Klimovskikh, I. I.; Otrokov, M. M.; Voroshnin, V. Y.; Sostina, D.; Petaccia, L.; Di Santo, G.; Thakur, S.; Chulkov, E. V.; Shikin, A. M. Spin–Orbit Coupling Induced Gap in Graphene on Pt(111) with Intercalated Pb Monolayer. *ACS Nano* **2017**, *11*, 368–374.
- (46) Martin, F. E.; Hensley, E. B. Photoelectric Emission from Barium Telluride. *Phys. Rev.* **1967**, *163*, 219–223.
- (47) Partin, D. L.; Thrush, C. M.; Clemens, B. M. Lead Strontium Telluride and Lead Barium Telluride Grown by Molecular-Beam Epitaxy. *J. Vac. Sci. Technol., B: Microelectron. Process. Phenom.* **1987**, *5*, 686–689.
- (48) Lu, G. H.; Huang, M.; Cuma, M.; Liu, F. Relative stability of Si surfaces: A first-principles study. *Surf. Sci.* **2005**, *588*, 61–70.
- (49) Zhang, H.; Ning, Y.; Yang, W.; Zhang, R.; Xu, X. Topological phase transition induced by $p_{x,y}$ and p_z band inversion in a honeycomb lattice. *Nanoscale* **2019**, *11*, 13807–13814.
- (50) Mostofi, A. A.; Yates, J. R.; Lee, Y. S.; Souza, I.; Vanderbilt, D.; Marzari, N. Wannier90: A Tool for Obtaining Maximally-Localised Wannier Functions. *Comput. Phys. Commun.* **2008**, *178*, 685–699.
- (51) Heyd, J.; Scuseria, G. E.; Ernzerhof, M. Hybrid Functionals Based on a Screened Coulomb Potential. *J. Chem. Phys.* **2003**, *118*, 8207–8215.
- (52) Nosé, S. A Unified Formulation of the Constant Temperature Molecular Dynamics Methods. *J. Chem. Phys.* **1984**, *81*, 511–519.